Jayanta Sinha
Research Scholar
Amity Institute of Aerospace Engineering
Amity University Uttar Pradesh, Noida
India

Sanjay Singh
Professor
Amity Institute of Aerospace Engineering
Amity University Uttar Pradesh, Noida
India

Om Prakash
Professor
Department of Aerospace Engineering
University of Petroleum and Energy Studies
Dehradun
India

Dhruv Panchal
Postgraduate Student
Amity Institute of Aerospace Engineering
Amity University Uttar Pradesh, Noida
India

Design Optimization of a Multi Row Disk Inlet Device with an Optimum Nose Cone Angle

The inlet is designed to compress the air and increase static pressure. In the present work, analyses have been carried out using 2D axisymmetric Reynolds averaged Navier Stokes equations (RANS) equations to capture the flow physics of the shock structure produced by the multi-row disk inlet device at different semi-cone angles. The present work involves numerical studies on the shock structure over the disk. Drag coefficient, pressure variation, and *vortex* behavior *with separation layers have been observed with various semi-cone angles of 12°, 15°, and 20° at the steady-state condition and zero angles of attack. At the free stream Mach number 2 and turbulence model k-ω SST, simulations have been carried out using commercial software. Compression through the cavity structure and the drag coefficient analysis at 20° shows better trade-off performance than the others. We also obtained that 20° is the maximum semi-cone angle for the current disk set-up and the operating conditions.*

Keywords: *Shockwaves, Mach Number, Supersonic Cavity Flow, Drag Coefficient, k-ω SST turbulence model*

1. INTRODUCTION

The design optimization of an inlet for modern supersonic aircraft is a challenging research topic of high interest. The supersonic inlet device must deliver high-pressure airflow to the engine's compressor over various operating conditions. Supersonic aircraft comp–ression systems typically require a series of movable compression ramps, porous walls, slots controlled by sophisticated software, and complex mechanical systems [1-3]. It is an admitted fact that to operate at an optimum design condition ($2 < M_\infty < 5$), the inlet device must produce a series of oblique shock waves followed by a terminal normal shock wave. This physical situ–ation is observed in mixed and internal compression inlets [4]. Multiple literature reviews [1-31] reveal that numerous studies were carried out on shock wave boundary layer interaction on the surface of the inlet device at the said operating conditions. These studies aimed to optimize the inlet device's design with a specific focus on flow separation and performance loss [4, 7, 9, 10, 12, 14, 29].

In order to improve the performance of supersonic aircraft, several strategies are recommended by the earlier investigators [2, 5, 6, 16, 20, 30]. One of the popular strategies is to use a variable geometry inlet. This solution was used, for example, in the Concorde aircraft, which used variable angle ramps. Same solution was also looked into for hypersonic vehicles [10, 12, 16, 20]. Some passive control approaches, such as using cavities with porous surfaces, can limit the effects of the flight Mach number [9, 10].

Fixed geometry inlets have disadvantages, like losses from operations at off-design conditions, structural integrity problems, separation layers' presence, stability issues, buzz phenomenon, flow distortion [31], and many others. So, facilitating the inlet device with the variable geometry is one of the options to overcome these issues [16, 21, 22]. Hiroaki Kobayashi [16], through experimental investigation, proposed an inlet device named a multi-row disk Inlet device (MRDID) for enhancing the performance of supersonic inlet devices [16, 22]. Figure 1 and 2 show the isometric views of the conventional center body and the multi-row disk inlet devices, respectively.

Multiple kinds of literature further reveal that though many studies have been carried out using different nose configurations [5, 16, 20, 22, 30], no studies have been carried out so far to capture the behavior of the shock structure produced by the multi-row disk (MRD) inlet device at different nose cone angles. Hence, the motivation behind this research paper is the variation of the flow physics with the change in nose cone angle and estimating the limit of the cone angle for a particular operating Mach. It is important to note that the modern multi-row disk technology makes it easy to get optimal performance in all operating conditions in supersonic aircraft by introducing the movable center body concept [16, 20, 22].

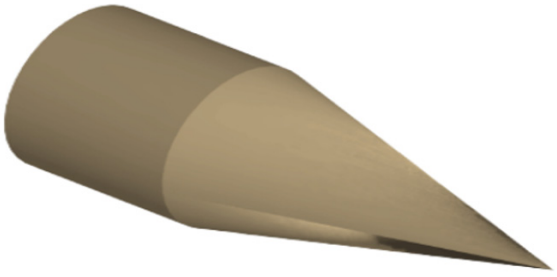

Figure 1. Conventional center body of the inlet

Received: September 2022, Accepted: December 2022
Correspondence to: Mr. Jayanta Sinha, Amity Institute of Aerospace Engineering, Amity University Uttar Pradesh, Sector 125, Noida, UP-201313, India
E-mail: jsinha1987@gmail.com
doi: 10.5937/fme2301023S
© Amity University Uttar Pradesh. All rights reserved

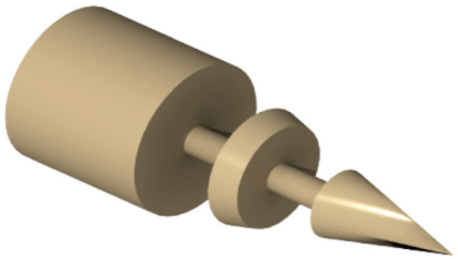

Figure 2. Center body with Multi-row disk

It is well known that capturing the shock structure over the MRD inlet is critical for its design optimization. The fact is that, in addition to the effect of back pressure, the configuration of the shock structure depends on the type of compression of the air inlet, viz., internal compression, external compression, and mixed compression. Mixed and internal types of inlets cause a series of oblique shock waves, followed by a weak normal shock wave. In the case of external compression, the normal shock is attached to the cowl [4]. Note that the normal shock location also depends on the effect of back pressure. In this paper, we focussed on parametric analytical studies to optimize the cone angle of the inlet based on the highest possible pressure ratio inside the cavity without inviting undesirable detached shock. The geometry of the cavity (1 < L/D <10) is selected based on the proper shear layer pattern, as shown in figure 3, as proposed by the previous investigators [18].

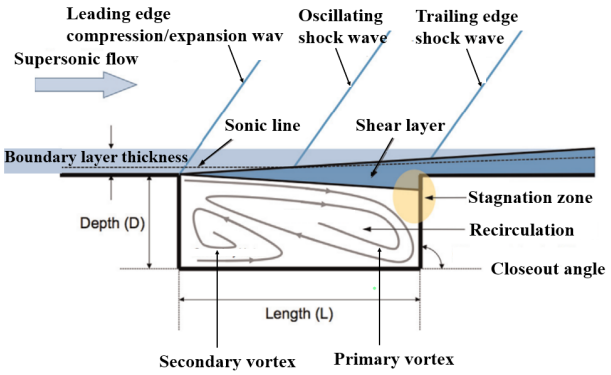

Figure 3. Basic geometric parameters and flow features of a cavity [18]

Figure 3 depicts the flow structure along the cavity and the flow behavior inside the cavity formed by the disks. The recirculation zone inside the cavity is sepa–rated from the supersonic freestream by a shear layer [5, 8, 18, 17, 23]. The shear layer drives trapped vortices in the recirculation zone, which are related to the cavity's size and strength. The cavity's leading and trailing edges and the shear layer produce unsteady waves that periodically behave like alternate shocks and expansion waves [17, 18]. The detailed phenomenon of the waves is explained by Heller and Delfs [19]. Cavities are classified based on the L/D ratio, where L is the length and D is the depth of the cavity. Three types are open, transitional, and closed cavities [10, 12, 21].

Open cavities have a shear layer bridging the length of the cavity, and closed cavities have a shear layer impinging and exiting from the base of the cavity [16, 21, 22, 23, 30]. Researchers have adopted several active and passive control techniques to suppress the adverse effects of complex flow inside the cavity [16, 20]. The passive techniques include front wall inclination, passive external bleed, and passive venting system. The active methods involve leading-edge microjet injection, piezoelectric bimorph actuators, etc. [5, 16, 21, 30].

Table 1. Types of cavities

Type of Cavity	L/D Ratio
Open	1<L/D<10
Transitional	10 ~14
Closed	L/D~>14

2. DEVELOPMENT OF DESIGN FOR THE MULTI ROW DISK INLET DEVICE

Figure 4 shows the typical oblique shock pattern over the surface of a center body of an inlet having a mixed-compression air inlet. Figure 5 depicts the altered pattern of the oblique shock waves when the center body is extended due to the movable option. It is evident from Fig.4 and Fig.5 that the center body of the inlet should be moved to adjust the shock pattern in accordance with the desirable performance of the inlet device [4, 6, 14]. Since this design option has significant stability issues and overall performance loss, optimizing movable inlet devices is inevitable. To overcome these issues, herein, we have carried out comprehensive numerical studies to optimize a multi-row disk inlet device for achieving an optimum semi-cone angle.

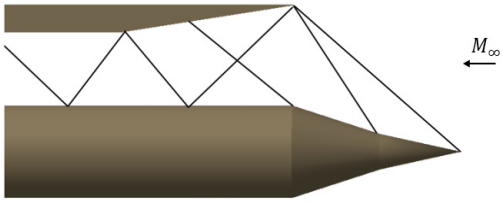

Figure 4. Contracted center body of the inlet

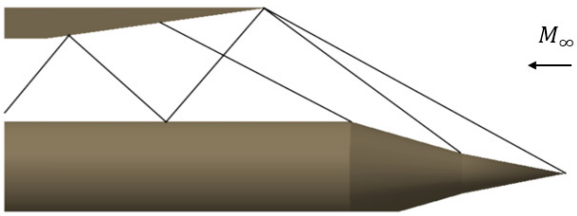

Figure 5. Extended center body of the inlet

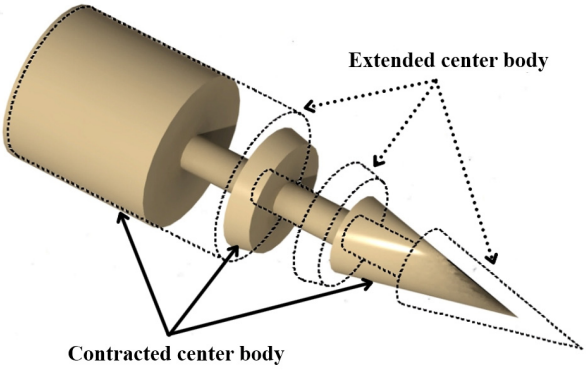

Figure 6. Concept of multi-row disk

The concept of the multi-row disk inlet device is shown in Figure 6, and the dashed line shows the extended portion of the center body. Multi-row disk inlet devices should be optimized based on the free-stream Mach number [15]. One of the optimization methods in this regard is the axial position adjustment of the center body, as shown in Figure 6. This device independently gives a more reliable mass flow ratio (MFR) and compression ratio [15, 19]. It has already been established that the disk's linear movement could alter the shock wave's location [5, 16, 22, 30] .

The center body is facilitated with a predesigned cavity so that the shear layer will bridge the length of the cavity and negate the adverse effect. The proposed model is designed based on the experimental and numerical studies of Koabayshi et al. [16, 20, 22] on MRD with multiple cavities with a single cone angle. In all these studies, the authors mainly focused on the boundary layer distortion at the inlet due to the presence of multi-row disks. We have conjectured that the optimization of the cone angle of the center body has a bearing on its performance owing to the fact that the shock wave will get detached at a higher cone angle [4] at the cruise condition (zero angles of attack). This physical situation leads to the underperformance of the vehicle due to the altered variations of the mass inflow. On this rationale, optimizing the cone angle of the center body for achieving the highest performance lucratively is inevitable. In order to examine the physical situation of the threshold of the detached shock wave generation, we have carried out comprehensive numerical studies with a wide range of semi-cone angles ($12 \leq \delta \leq 23$). The numerical methodology is discussed in the subsequent section. In this paper, we have reported the data only for four different semi-cone angles, including two extreme angles i,e. δ=12° & 23° and two intermediate angles i,e. δ=15° & 20°

3. THE NUMERICAL METHODOLOGY

The simulations have been carried out using validated steady state, two-dimensional (2D), and an implicit Reynolds-averaged Navier-Stokes equations (RANS) solver with *k-ω SST* turbulence model. The solver is verified using benchmark data from a closed-form ana–lytical model [24-26]. Furthermore, numerical results are validated using benchmark data [24-27] for various operating conditions. Data Presented by Gholap et al. [25] and Tembhurnikar et al. [27] have been specifi–cally used to validate the numerical turbulence model.

Since, no experimental work has been undertaken in support of the present research work, we have validated the work using the published paper by Milicev [32] and Damljanović et al. [33]. The off-design performance of the model in the wind tunnel has been studied based on the work of Damljanović et al. [34]

Figure 7 shows the idealized 2D physical model of the multi-row-disk (MRD) selected herein for the parametric studies. Geometrical details of four different cases of MRD with four different semi-cone angles with identical cavities (i.e., same L/D ratio) are given in Table 2. The total length of the center body (L) is fixed as constant (100 mm) in all four cases. Note that while altering the semi-cone angle, the geometrical variables in the radial direction will be altered to maintain the identical cavity size to meet the design objective of the MRD. These variations are reflected in Table 2.

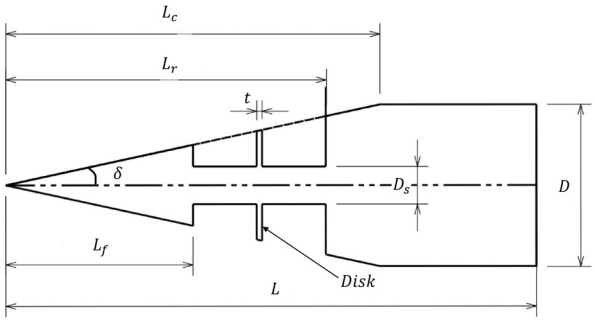

Figure 7. Drafting of the geometry

Table 2. Dimensions of the geometry

	Type 1	Type 2	Type 3
L_f	35.29	35.29	35.29
L_c	70.5	70.5	70.5
D	30	37.78	51.32
L_r	60.29	60.29	60.29
t	1	1	1
D_s	6.95	10.91	17.69
L	100	100	100
δ	12°	15°	20°

Inlet far-field boundary is fixed at a distance of 2L from the tip of the center body of the inlet. Figure 8 shows the upper half of the physical model and the optimized computational domain. Figure 8 shows the grid system in the full computational domain with the enlarged view of the grid system selected for the predesigned cavity.

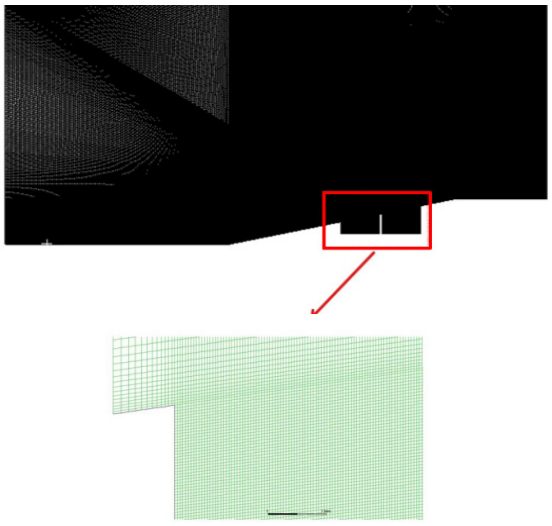

Figure 8. Computational grid with zoomed view near the cavities

Grid system is selected after detailed grid refinement exercises (see Fig. 9). We started with a coarse mesh with 1.5 lacs cells, followed by medium quality mesh with 2.5 lacs cells, and then a fine mesh with 3.5. lastly, we used a super fine mesh having 5 lacs cells. After multiple iterations, we selected a fine mesh consisting

of 3.5 lac cells instead of the superfine mesh to reduce the computational time for the parametric studies. In all cases, the inlet Mach number is imposed as 2.0, and the inlet pressure is selected as 39468.56 Pa, with the corresponding temperature of 167K based on the published paper [5]. Note that we have obtained the anticipated oblique shock wave pattern at the tip of the center body with a fine mesh grid system, as shown in the upper part of Fig. 9.

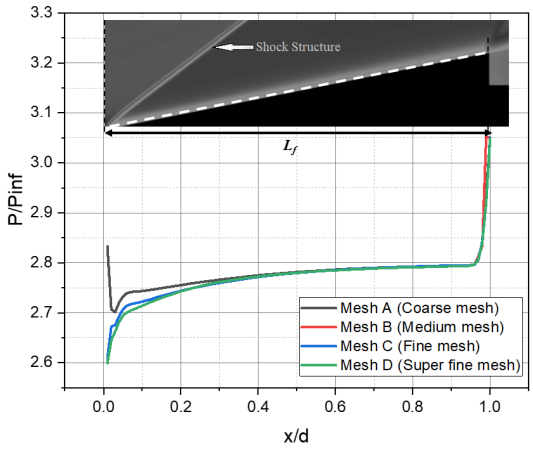

Figure 9. Grid independent test

To capture the flow behavior, a large fluid domain has been created and the details about the domain are shown in figure 10. The solver setup is shown in Table 3. Table 4 shows the inlet conditions that are used for the simulation.

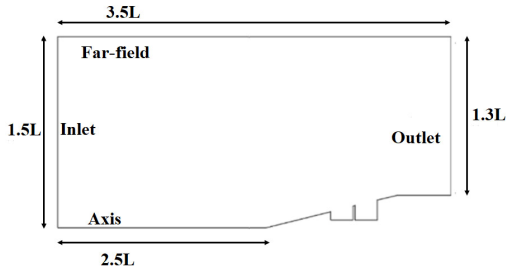

Figure 10. Named selections for simulation

Table 3. Solver setup

Scheme/parameters	Type/quantities
Solver precision	Double precision
Solver type	Density-based implicit, steady state
RANS	k-ω SST (2 PDE model)
Inviscid flux scheme	Roe flux-difference splitting scheme64
Spatial discretization	Second-order upwind scheme
Gradient evaluation	Least squares cell-based

Boundary conditions have been used based on the data provided by Sinha, J. et al. [5, 21, 30]. Preliminary grid validation has also been carried out based on the data provided in [16, 22] and has already been published [5].

4. RESULTS AND DISCUSSION

In this manuscript, we have carried out comprehensive numerical studies for the cone angle optimization of multi row disk (MRD) for modern aircraft engines flying at a Mach number of 2.0. The numerical simulations have been carried out using validated steady, two-dimensional (2D), an implicit Reynolds-averaged Navier-Stokes equations (RANS) solver with *k-ω SST* Turbulence model. The numerical results gene–rated for four different cases are depicted in Figs. 11-18. It is quite clear from the density contours (see Figs. 11-13) that the anticipated oblique shock waves are generated over the cavities where the shear layer effects are evident. The shear layer pattern is highlighted in Fig. 11 as a numerical schileren (see bottom half of Fig. 11). The density contours are compared with the numerical schlieren images for different semi-cone angles. It is evident from these figures that the oblique shock wave angle increases with an increase in the semicon angle. Analytically we have calculated through the θ-β-M relation that the oblique shock wave will detach at a higher semicon angle (δ>22°). Therefore, we have car–ried out a numerical simulation to capture the threshold of shock detachment in the axisymmetric mode and the flow physics of attached and detached oblique shock waves at a wide range of semicon angle (12≤δ≤23°). Fig. 11-13 shows the changes in the shock structure due to the changes in the semicon angles. Effects are quite prominent at the rear walls of the first and second cavities.

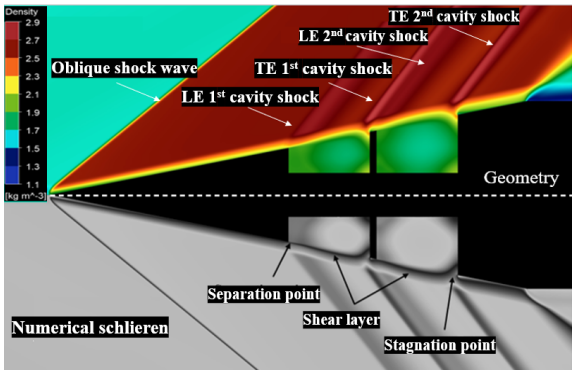

Figure 11. Density contour and numerical schlieren for AC012

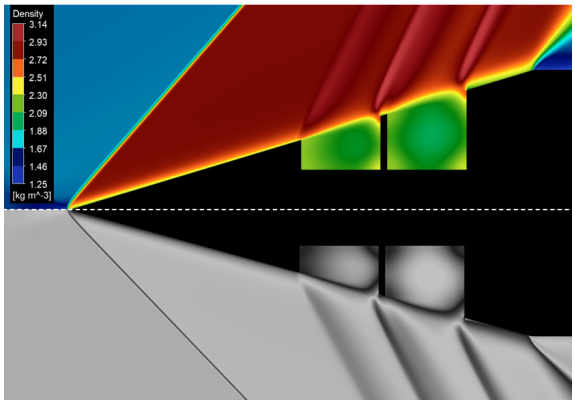

Figure 12. Density and numerical schlieren contour for AC015

As shown in Figure 14, the effect of eddy viscosity, shear layer, shed layer (see Fig 16), and vortex struc–tures have been captured. Contour lines are quite useful in determining the comprehensive summary of cavity flow. Single vortical structures are more dominant for the first and second cavities of axisymmetric cone angle of 12° (AC012), whereas small eddies can be seen near the front walls. The oscillating shear layer is present in both cavi–

ties. Mass diffusion into and out of the cavity across the shear is also quite evident at the rear wall of the 2nd cavity.

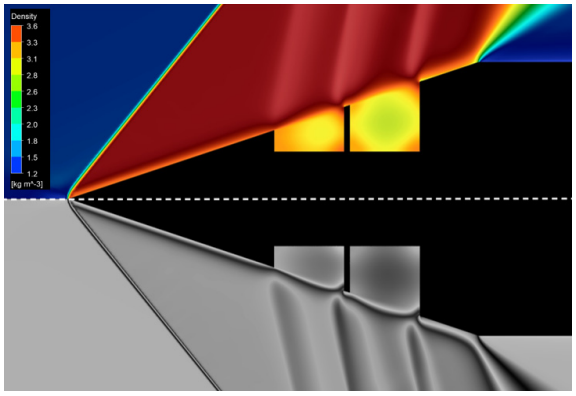

Figure 13. Density and numerical schlieren contour for AC020

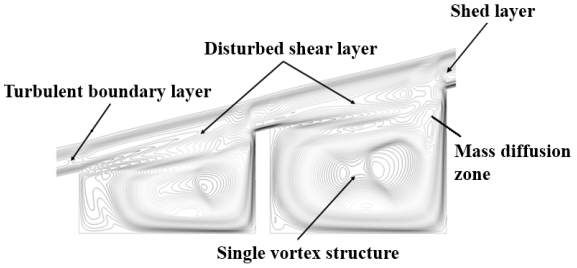

Figure 14. Eddy viscosity effect on AC012

Figures 15, 16, and 17 show the Mach number contour coupled with the streamlines for various semi-cone angles to explain the flow physics. A sonic line has been captured near the wall boundary, just over the cavity. This sonic line acts as a separation layer which, when extended over the cavity, becomes the shear layer. Below the separation layer, the Mach number is subsonic, and recirculation is accrued. The shed layer is also captured near the rear walls of the cavity, which is also observed in all the figures. Figure 18 shows the Mach number contour for AC023, the shock is detached because the deviation angle is greater than the maximum achievable deviation angle for an attached oblique shock. For the geometry used in the present case, the critical angle is 20°. Further increment in the semi-cone angle will lead to detached shock and a large level of unsteadiness, which is undesirable. So, in the present study, we have also achieved the limit of the critical semi-cone angle.

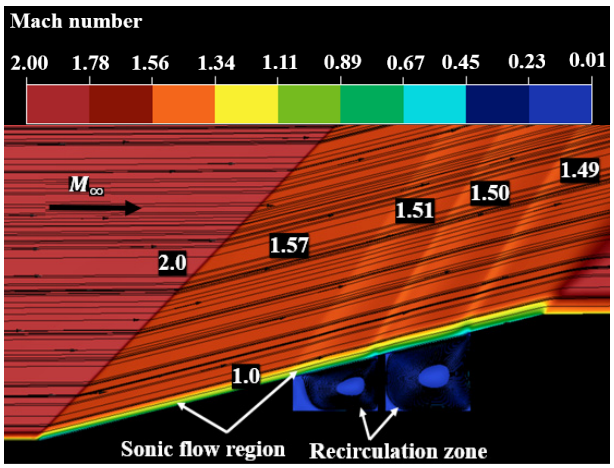

Figure 15. Mach number contour along with streamlines for AC012

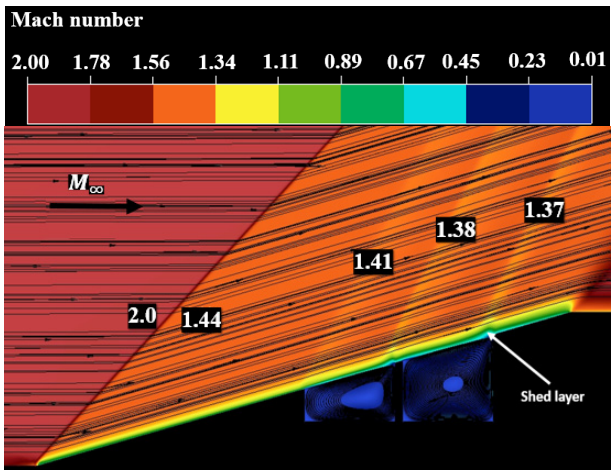

Figure 16. Mach number contour along with streamlines for AC015

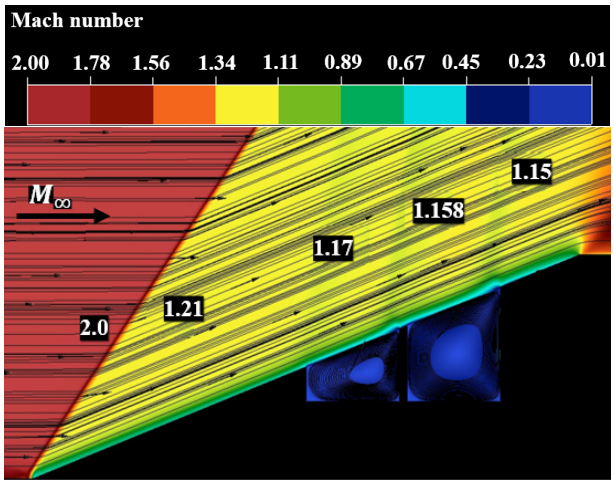

Figure 17. Mach number contour along with streamlines for AC020

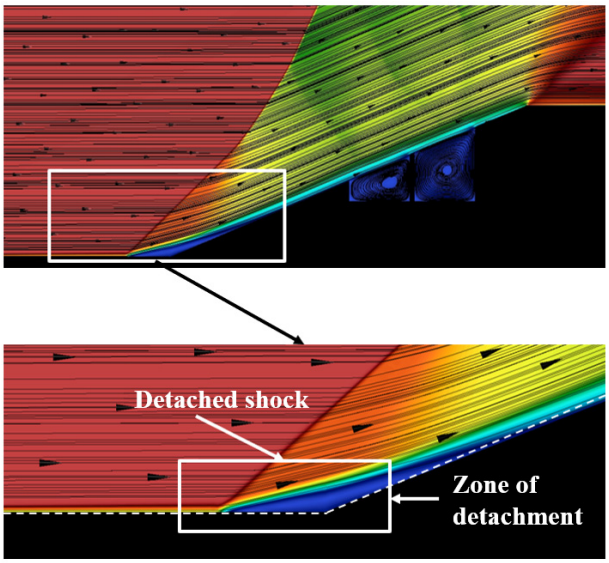

Figure 18. Mach number contour along with streamlines for AC023

Hence we restricted this research only up to the 20° semi-cone angle and didn't go into the details of flow physics of the 23° semi-cone angle case. Pressure distribution along the front wall of both the first cavity and the second cavity for the different cone angles, as given in Figure 19, doesn't show large differences.

However, as the cone angle increases from 12° to 20°, the pressure ratio increases from 1 to 3. Spike in the ratio can be attributed to the increasing shock strength. At mid of y/d, P/Pinf for the front wall almost approaches each other for ACθ12. However, the value of P/Pinf along ACθ15 shows a contrasting result.

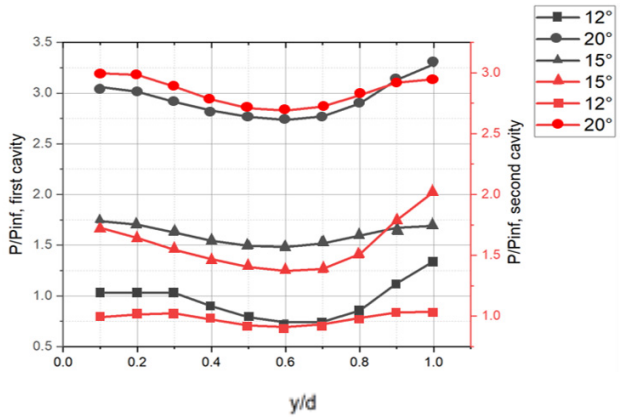

Figure 19. Pressure variation along the front wall of cavities

Variation in non-dimensionalized pressure about the rear wall shows the increase in pressure ratio as we move up from the cavity bottom to the tip. For all three cases, a peak pressure can be obtained at around y/d =0.9, which is the shock impingement point. This pressure ratio is highest for ACθ20 near the tip of the cavity. The pressure level is also higher for the second cavity than for the first cavity.

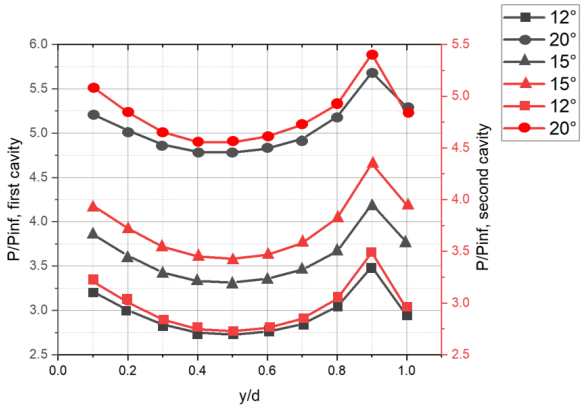

Figure 20. Pressure variation along the rear wall cavities

The pressure plots shown in Figure 20 for the first and second cavity rear walls show that the pressure variation is quite smooth, and the pressure slightly drops near the center of the rear wall. However, the trend of increasing pressure with the increase in cone angle is also visible in the graph.

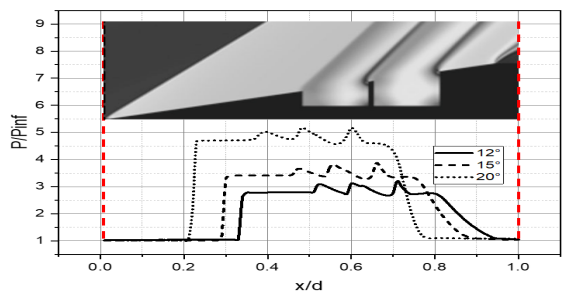

Figure 21. Pressure variation along the cavity length

Figure 21 has been generated to understand better the pressure distribution rise across the total length of all three cone-angle geometries. The length ranges from the tip of the nose-cone to the end of the MRDID. The length and the pressure are both non-dimensionalized. Data has been captured along the line 2mm above the rear horizontal surface. Let's analyze the three outcomes of pressure variation at a similar height. We can see that for high semi-cone angles, compression wave through the front and rear shock wave is more significant compared to low semi-cone angle, and ACθ20 semi-cone model gives better compression through the cavity shocks as compared to ACθ12 and ACθ15. The drag coefficient increases with the cavity cone angle as well. From Table 2 we can see that the drag coefficient is maximum for ACθ20 and minimum for ACθ12.

Table 4. Variation of drag coefficient with semi-cone angle

Semi cone angle	Drag coefficient
12°	0.0057
15°	0.0086
20°	0.018

5. CONCLUSION

The numerical schlieren has properly captured all the fundamentals, flow features, shear layer, sonic line, shed layer, and other cavity flow features. The shear layer distortion increases with the increase in the semi-cone angle. Because of the strong shock wave inte–raction at a high semi-cone angle, the overall cavity internal pressure is also high. The pressure rise due to impingement shock on the 2nd cavity is higher than the 1st cavity by almost 5-10%, which also indicates that the presence of a large number of tandem cavities for–med by more disks will make the flow unfavorable from the structural point of view. Hence, the structural ana–lysis will also be important for the feasibility of these types of inlets. Structure analysis will be undertaken in the second part of this paper. Here the drag coefficient obtained for different semi-cone angles follows the increasing trend from ACθ12 to ACθ20. Drag coefficient has increased to almost 3 times. Pressure on the MRDID also increases from ACθ12 to ACθ20, which is almost two times. Now, when we select the air-intake system, the focus is always on the high-pressure compression inside the inlet. Drag can, however, be reduced through the improvement in the aerodynamics of the aircraft, and the performance can be enhanced by optimizing the nozzle design. Lot of literature is on enhancing the aerodynamic efficiency of the supersonic aircraft. Hence, from the air-intake perspective, we will give paramount importance to the semi-cone angle, which provers high compression. Hence, the comp–ression data shows that the ACΘ20 is better than the other two designs, based on its application as a part of mrdid. We have also obtained the limit for the maxi–mum semi-cone angle, which will act as the indicator of the maximum pressure compression that can be obtained from this configuration, based on the given set of disks. More studies on the disks will give a clear picture of the flow distortion.

ACKNOWLEDGMENT

The authors would like to sincerely thank all the faculty and staff members of Amity Institute of Aerospace Engineering, Amity University Uttar Pradesh for their support during this research work.

REFERENCES

[1] Gridley, M.C., Walker, S.H.: Advanced Aeroengine Concepts and Controls, *AGARD Conf. Proc. 572, 86th Symposium, Seattle*, WA, USA, 1996.

[2] Valorani, M., Nasuti, F., Onofri, M., Buongiorno, C.: Optimal supersonic intake design for air col–lection engines (ACE). Acta Astronaut. Vol. 45, pp.729–745, 1999.

[3] Ran, H. and Mavris, D.: Preliminary design of a 2D supersonic inlet to maximize total pressure recovery. In Proceedings of the AIAA 5th ATIO and 16th Lighter-Than-Air Sys Tech. and Balloon Systems Conferences, Arlington, VA, USA, pp. 26–28, September 2005.

[4] Seddon, J., Goldsmith, E.L.: *Intake Aerodynamics*, 2nd Edn., Blackwell Science 1999.

[5] Jayanta Sinha, J., Arora, K., Prakash, O., Bandopadhyay S., Saha, P. and Bhattacharya, A.: Analysis of multi row disk inlet device in super–sonic flow condition, *21st Annual CFD Symposium*, August 2019, Bangalore, India.

[6] Surber, L., Tinapple, J.: Inlet flow control technology: Learning from history, reinventing the future. In Proceedings of the *50th AIAA Aerospace Sciences Meeting Including the New Horizons Forum and Aerospace Exposition*, 9–12 January 2012, Nashville, TE, USA, pp. 12.

[7] Dissimile, P.J.: Effect of planform aspect ratio on flow oscillations in rectangular cavities. J. Fluids Eng. Vol. 122, pp. 32–38, 2000

[8] Stallings, R.L. and Wilcox, F.J.: Experimental cavity pressure distribution at supersonic speeds. NASA TP 2683, 1987.

[9] Humrutha. G, Kaushik, M., and Sinhamahapatra K.P.: Shock Boundary Layer Interaction Control in Supersonic Intake using Cavity with Porous Surface., *35th AIAA Applied Aerodynamics Conference*, 2017, Denver, Colorado.

[10] Wei, H., Han, W., Yan-guang, Y., Li, Y., and Shi-bin, L.: Recent advances in the shock wave/boundary layer interaction and its control in internal and external flows, Acta Astronautica, Vol. 174, pp.103-122, 2020.

[11] Aradag, S., Gelisli, K.A, and Yaldir, E.C.: Effects of Active and Passive Control Techniques on Mach 1.5 Cavity Flow Dynamics, Hindawi Int. J. of Aerospace Engineering Volume 2017, Article ID 8253264, 2017.

[12] Gunasekaran, H., Thangaraj, T., Jana, T., Kaushik, M.: Effects of Wall Ventilation on the Shock-wave/Viscous-Layer Interactions in a Mach 2.2 Intake. Processes, Vol. 8, No. 2, Article No. 208, 2020.

[13] Sorensen, N.E., Latham, E.A. and Semltzer, D.B.: Variable geometry for supersonic mixed-compression inlets, NASA Ames research center, Moffett field, Calif, Vol. 13, no 4, April 1976.

[14] Kotteda, V.M.K., and Mittal, S.: Viscous flow in a mixed compression intake, International Journal for Numerical Methods in Fluids, Vol. 67 No. 11, pp.1393 – 1417, 2010.

[15] Kopasakis, G., Connolly, J.W., Paxson, D.E. and Woolwine, K.J.: Quasi 1D Modeling of Mixed Compression Supersonic Inlets, AIAA 2012-0775, 2012.

[16] Kobayashi, H., Nobuhiro, T., Sato, T., Maru, Y. and Kojima, T.: Experimental study of multi-row disk inlets for hypersonic air-breathing propulsion. *42nd AIAA Aerospace Sciences Meeting and Exhibit*, 5 - 8 January 2004, Reno, Nevada 2004. AIAA 2004-861.

[17] Karthik, S.K.: Shock and shear layer interactions in a confined supersonic cavity flow, Physics of Fluids, Vol. 33, Issue: 06, 2021.

[18] Barnes, F.W. and Segal, C.: Cavity-based flame holding for chemically-reacting supersonic flows, Progress in Aerospace Sciences, Vol. 76, pp. 24–41, 2015.

[19] Heller, H.H., and Delfs, J.: Cavity pressure oscillations: the generation mechanism visualized, J. Sound Vib. Vol. 196 No. 2, pp. 248–252, 1996.

[20] Hiroaki, K., Maru, Y. Hongoh, M., Takeuchi, S., Okai, K. and Kojima, T.: Study on variable-shape supersonic inlets and missiles with MRD device. Acta Astronautica Vol. 61, pp. 978 –988. 2007

[21] Sinha, J.: Studies on the Transition of the Flow Oscillations over an axisymmetric open cavity model. Advances in Aerospace Science and Applications, Vol.3, 2013.

[22] Kobayashi, H., Kojima, T., Okai, K. and Maru, Y.: Study of Supersonic Cavity Flow in Advanced Variable Geometry Inlet, *55th International Astronautical Congress* Vancouver, Canada. 2004.

[23] Tam, C. J., Orkis, P. D., and Disimile, P. J.: Algebric turbulence model simulations of

[24] supersonic open cavity flow physics. AIAA Journal, Vol. 34 No. 11, pp.2255-2260, 1996.

[25] Sanal Kumar, V.R., Sankar, V., Nichith, C., Saravanan, V., et al.: A closed-form analytical model for predicting 3D boundary layer displacement thickness for the validation of viscous flow solvers, AIP Advances, Vol. 8, Issue: 02, Article No. 025315, 2018.

[26] Gholap, T.B., Salokhe, R.V., Ghadage, G.V., Mane S.V., and Sahoo, D.: Aerodynamic Analysis of an AK-47 Bullet Moving at Mach 2.0 in close proximity to the Ground, FME Transactions, Vol. 50, No. 2, pp. 369-381, 2022.

[27] Taha, A.A., Tiwari, S.N., and Mohieldin, T.O.: Validation of fluent CFD code in supersonic flow fields, *15th AIAA Computational Fluid Dynamics Conference*, 2001, Anaheim CA, AIAA 2001-2637

[28] Tembhurnikar, P.V., Jadhav, A.T. and Sahoo, D.: Effect of Intermediate Aerodisk Mounted Sharp Tip Spike on the Drag Reduction over a Hemispherical Body at Mach 2.0, FME Transactions, Vol. 48, pp. 779-786, 2020.

[29] Sridhar, V., Gai, S. L., and Kleine, H.: A Numerical investigation of supersonic cavity flow

[30] at Mach 2. *18th Australasian Fluid Mechanics Conference*, Launceston, Australia, 2012.

[31] Babinsky, H., Li, Y. and Pitt Ford, C. W.: Microramp control of supersonic oblique shockwave/boundary-layer interactions, AIAA Journal, Vol. 47, No. 3, pp. 668–675, 2009.

[32] Siddhant Khurana, Gopan Gopalan Achary, Saksham Arora and Jayanta Sinha.: Computational Analysis of Multi Row Disk Inlet, *First International Conference on Recent Advances in Aerospace Engineering (ICRAAE)*, 2017, India

[33] Migliorini, M., Zachos, P.K. and MacManus, D.G.: Novel Method for Evaluating Intake Unsteady Flow Distortion, J. Propulsion and Power, Vol. 38, No.1, 2022.

[34] Milićev, SS.: An Experimental Study of the Influ–ence of Spike in Supersonic and Transonic Flows Past a Hemispheric Body, FME Transactions, Vol. 50, No. 1, PP. pp. 24-31, 2022.

[35] Damljanović, D., Vuković, D., Ocokoljić, G., Rašuo, B.: Convergence of Transonic Wind Tunnel Test Results of the AGARD-B Standard Model, FME Transactions, Vol. 48, No. 4, pp. 761-769, 2020.

[36] Damljanović, D., Vuković, Đ., Ocokoljić, G., Ilić B., Rašuo, B.: Wind Tunnel Testing of ONERAM, AGARD-B and HB-2 Standard Models at Off-Design Conditions, Aerospace, Vol. 8, No. 10, 275, 22 Sep. 2021.

NOMENCLATURE

P	Pressure
Pinf	Free stream pressure
δ	Semi-cone angle
L	Length of the first cavity
D	Depth of the first cavity
k-ω SST	k-ω shear stress transport
ACθ12	Axisymmetric semi-cone angle of 12°
ACθ15	Axisymmetric semi-cone angle of 15°
ACθ20	Axisymmetric semi-cone angle of 20°
MRDID	Multi-row disk inlet device
CFD	Computational fluid dynamics
PDE	Partial differential equation
MFR	Mass flow rate ratio
x/D	Ratio of horizontal length upon the depth of the cavity
y/D	Ratio of vertical length upon the depth of the cavity
LE	Leading edge
TE	Trailing edge

ОПТИМИЗАЦИЈА ДИЗАЈНА ВИШЕРЕДНОГ УЛАЗНОГ ДИСКА СА ОПТИМАЛНИМ УГЛОМ НОСНОГ КОНУСА

Ј. Сина, С. Синг, О. Пракаш, Д. Панчал

Улаз је дизајниран да компримује ваздух и повећава статички притисак. У овом раду, анализе су спроведене коришћењем 2Д осносиметричних Реинолдсових усредњених једначина Навиер Стокеса (РАНС) да би се ухватила физика струјања ударне структуре коју производи вишередни диск улазни уређај под различитим угловима полуконуса. Овај рад обухвата нумеричке студије структуре шока преко диска. Коефицијент отпора, варијација притиска и понашање вртлога са сепарационим слојевима примећени су са различитим угловима полуконуса од 12°, 15° и 20° у стабилном стању и нултим угловима напада. Код слободног тока Маховог броја 2 и модела турбуленције к-ω ССТ, симулације су спроведене коришћењем комерци–јалног софтвера. Компресија кроз структуру шуп–љине и анализа коефицијента отпора на 20° показују боље перформансе компромиса од осталих. Такође смо добили да је 20° максимални угао полуконуса за тренутно подешавање диска и услове рада.